Optics Letters

Experimental study of reducing beam wander by modulating the coherence structure of structured light beams

Jiayi Yu,[1,2] Xinlei Zhu,[2] Fei Wang,[2] Dongmei Wei,[1] Greg Gbur,[3,4] and Yangjian Cai[1,2,5]

[1]*Shandong Provincial Engineering and Technical Center of Light Manipulations & Shandong Provincial Key Laboratory of Optics and Photonic Device, School of Physics and Electronics, Shandong Normal University, Jinan 250014, China*
[2]*School of Physical Science and Technology, Soochow University, Suzhou 215006, China*
[3]*Department of Physics and Optical Science, University of North Carolina at Charlotte, Charlotte, North Carolina 28223, USA*
[4]*e-mail: gjgbur@uncc.edu*
[5]*e-mail: yangjiancai@suda.edu.cn*

We study the beam wander of a class of structured light beams, Hermite–Gaussian correlated Schell-model (HGCSM) beams, in theory and in experiment. It is found that modulating the coherence structure of a structured light beam can reduce the turbulence-induced beam wander, i.e., a HGCSM beam with larger mode orders or lower coherence experiences smaller beam wander. Our experimental results are consistent with theoretical predictions, and the insights here suggest that HGCSM beams could be useful in free-space optical communications. © 2019 Optical Society of America

It is well known that a laser beam will experience random perturbations in amplitude and phase when it propagates through a turbulent atmosphere, due to fluctuations of the refractive index caused by stochastic variations of temperature [1]. Accordingly, the instantaneous center of a laser beam will randomly displace in the receiver plane, an effect known as beam wander [1,2]. Beam wander is a significant limitation in applications such as free-space optical communication [3], global quantum communication [4], and laser guide stars [5]; thus, it is imperative to overcome or reduce its influence.

Researchers have long recognized that partially coherent beams (PCBs) can have lower turbulence-induced beam wander than their fully coherent counterparts [6–9]. An experimental study of the beam wander of a Gaussian Schell-model (GSM) beam was reported in Ref. [7]. The resistance of PCBs to turbulence is often explained by using coherent mode representation [10,11]. The beam wander of various partially coherent beams in turbulent atmosphere has been widely investigated, and several strategies have been introduced to reduce beam wander, e.g., modulating the PCBs with non-trivial beam profiles [12], phases [9,13], and polarization [14].

In addition, coherence structure manipulation as a new method for generating novel structured light beams has attracted a great deal of attention [15,16]. Laser beams with nonconventional correlation functions (Schell-model functions with non-Gaussian correlation) can be achieved by coherence structure manipulation and display some extraordinary propagation properties [15–21]. More significantly, these new classes of beams show stronger resistance to turbulence than traditional GSM beams [20–24]. To date, few papers have studied the beam wander properties of structured light beams with nonconventional correlation functions [9], and none has studied the application of coherence structure in reducing turbulence-induced beam wander in both theory and experiment. In this Letter, we theoretically and experimentally study the beam wander of structured light beams, choosing Hermite–Gaussian correlated Schell-model (HGCSM) beams as an illustrative example.

Beam wander can be expressed as the variance of random displacement of the instantaneous beam center as it propagates through atmospheric turbulence. A model of beam wander of coherent beams valid under general weak turbulence conditions is given by Andrews and Phillips as [1]. In 2012, the theory was extended to the case of partially coherent beams [25]:

$$\langle r_c^2 \rangle = 4\pi^2 k^2 W_{FS}^2 \int_0^L \int_0^\infty \kappa \Phi_n(\kappa) H_{LS}(\kappa, z)$$
$$\times \left\{ 1 - \exp\left[-\frac{\Lambda L \kappa^2 (1 - z/L)^2}{k} \right] \right\} d\kappa dz, \quad \text{(1)}$$

where $k = 2\pi/\lambda$ is the wavenumber, with λ being the wavelength, L is the total propagation path length, and z is the distance of an intercept point from the input plane at $z = 0$. The function $\Phi_n(\kappa)$ is the atmospheric spectrum, where κ denotes spatial frequency. The quantity W_{FS} is the beam width at the receiver plane in free space, and $\Lambda = 2L/kW_{FS}^2$. The quantity $H_{LS}(\kappa, z) = \exp(-\kappa^2 W_{LT}^2)$ is a large-scale filter function, and W_{LT} is the long-term beam width in the presence of turbulence, to be discussed in more detail momentarily.

Here, for ease of calculation, Eq. (1) is simplified by applying the geometrical optics approximation, also discussed in Ref. [1]. In this approximation, diffraction effects are neglected, and the last term in the above equation becomes

$$1 - \exp\left[-\frac{\Lambda L \kappa^2 (1-z/L)^2}{k}\right] \approx \frac{\Lambda L \kappa^2 (1-z/L)^2}{k}, \qquad L\kappa^2 \ll k.$$

(2)

We model the turbulence using the von Karman power spectrum, which can describe Kolmogorov ($\alpha = 11/3$) and non-Kolmogorov ($\alpha \neq 11/3$) power spectra and takes into account both inner and outer scales:

$$\Phi_n(\kappa) = A(\alpha)(\kappa^2 + \kappa_0^2)^{-\alpha/2} C_n^2 \exp(-\kappa^2/\kappa_m^2), \qquad \textbf{(3)}$$

where C_n^2 is a generalized refractive-index structure parameter with units $m^{3-\alpha}$, $\kappa_0 = 2\pi/L_0$, with L_0 being the outer scale of turbulence, $\kappa_m = c(\alpha)/l_0$, with l_0 being the inner scale of turbulence. The quantities $A(\alpha)$ and $c(\alpha)$ are defined in Ref. [24].

With the geometrical optics approximation and a model of turbulence, we can integrate Eq. (1) and obtain a formula for the beam wander in non-Kolmogorov turbulence:

$$\langle r_c^2 \rangle = \frac{4\pi^2 C_n^2 A(\alpha) L^2}{(\alpha-2)} \kappa_0^{-\alpha} \int_0^L \left(1-\frac{z}{L}\right)^2$$

$$\times \left\{ -2\kappa_0^4 + \kappa_0^\alpha \kappa_m^2 (W_{LT}^2 + \kappa_m^{-2})^{\alpha/2}(1+\kappa_m^2 W_{LT}^2)^{-2} \right.$$

$$\times [2\kappa_0^2(1+\kappa_m^2 W_{LT}^2) + (\alpha-2)\kappa_m^2]\exp\left[\left(\frac{\kappa_0}{\kappa_m}\right)^2 + \kappa_0^2 W_{LT}^2\right]$$

$$\left. \times \Gamma\left[2-\frac{\alpha}{2}, \left(\frac{\kappa_0}{\kappa_m}\right)^2 + \kappa_0^2 W_{LT}^2\right] \right\} dz,$$

(4)

and $\Gamma(\cdot)$ represents the Gamma function. Equation (4) is a general formula of beam wander for an arbitrary laser beam propagating in non-Kolmogorov turbulence. It is striking to note that the beam wander depends on the source parameters, i.e., the only parameters we can control, only through the long-term beam width W_{LT}. Any change to the source parameters that affects W_{LT} will consequently affect beam wander, and W_{LT} can depend on these parameters in a non-trivial way. The quantity W_{LT}^2 can be described as the mean-squared beam width of a laser beam propagating in turbulence [26].

We now focus on the specific example of HGCSM sources. In the Cartesian coordinate system, the cross-spectral density function of a HGCSM beam in the source plane is expressed as [19,24]

$$W(\mathbf{r}_1, \mathbf{r}_2) = G_0 \exp\left(-\frac{\mathbf{r}_1^2 + \mathbf{r}_2^2}{4\sigma_0^2}\right) \mu(\mathbf{r}_2 - \mathbf{r}_1), \qquad \textbf{(5)}$$

where $\mathbf{r}_1 \equiv (x_1, y_1)$ and $\mathbf{r}_2 \equiv (x_2, y_2)$ are two arbitrary transverse position vectors in the source plane, G_0 is a constant, and σ_0 denotes the beam width. The function $\mu(\mathbf{r}_2 - \mathbf{r}_1)$ represents the degree of coherence (DOC) of the beam and is given by [19,24]

$$\mu(\mathbf{r}_2 - \mathbf{r}_1) = \frac{H_{2m}[(x_2-x_1)/\sqrt{2}\delta_{0x}]}{H_{2m}(0)} \exp\left[-\frac{(x_2-x_1)^2}{2\delta_{0x}^2}\right]$$

$$\times \frac{H_{2n}[(y_2-y_1)/\sqrt{2}\delta_{0y}]}{H_{2n}(0)} \exp\left[-\frac{(y_2-y_1)^2}{2\delta_{0y}^2}\right], \qquad \textbf{(6)}$$

with δ_{0x} and δ_{0y} being the transverse coherence widths along x and y directions, respectively. Here, H_m denotes the Hermite polynomial of order m.

The mean-squared width of this beam in non-Kolmogorov turbulence was obtained as Eq. (33) in our previous study (see Ref. [24]) and can be expressed as

$$W_{LT}^2 = \langle \rho^2 \rangle = \frac{z^2}{\delta_{0x}^2 k^2}(2m+1) + \frac{z^2}{\delta_{0y}^2 k^2}(2n+1)$$

$$+ \frac{z^2}{2k^2\sigma_0^2} + 2\sigma_0^2 + \frac{4\pi^2 z^3}{3} T, \qquad \textbf{(7)}$$

with m and n being the beam orders along x and y directions, respectively. T is a turbulence parameter, which can be written as $T = \int_0^\infty \kappa^3 \Phi_n(\kappa) d\kappa$. It is to be noted from this expression that W_{LT} is larger for higher beam orders and lower spatial coherence.

Applying Eqs. (4) and (7), we can study the beam wander of HGCSM beams in non-Kolmogorov turbulence. Generally, the root-mean square (RMS) of the centroid of a laser beam in the receive plane is used to express beam wander, as in Ref. [1]. Now, we will study the RMS of the centroid of HGCSM beams through non-Kolmogorov turbulence based on the above equations. In the following numerical examples, the parameters of the beam and the turbulence are set as $\lambda = 632.8$ nm, $\sigma_0 = 2.5$ mm, $L_0 = 1$ m, $l_0 = 1$ mm, $C_n^2 = 5 \times 10^{-13}$ m$^{-2/3}$, $\alpha = 11/3$, and $\delta_{0x} = \delta_{0y} = \delta_g$, and the propagation path length is $L = 2.5$ m. For these parameters, the Rytov variance $\sigma^2 = 0.00048 \ll 1$, which satisfies the condition of weak turbulence.

Figure 1 reveals the beam wander of HGCSM beams versus the coherence length δ_g for different values of the beam orders m and n with $C_n^2 = 5 \times 10^{-13}$ m$^{-2/3}$. We find from Fig. 1 that the value of the beam wander increases rapidly as δ_g is increased from zero, and then asymptotically approaches a fixed value in the coherent limit ($\delta_g \to \infty$). We also find that the beam wander of HGCSM beams is smaller than that of traditional GSM beams ($m = n = 0$). Furthermore, the magnitude of the beam wander decreases with increasing beam orders, which means the fluttering of the beam spot is less dramatic with large beam orders. Thus, we have confirmed that HGCSM beams with larger beam orders and/or lower coherence exhibit a stronger turbulence resistance.

Figure 2 shows the beam wander of HGCSM beams versus the generalized refractive-index structure parameter C_n^2 for different values of beam orders m and n, for a fixed coherence width $\delta_g = 0.17$ mm. This value was taken to compare with
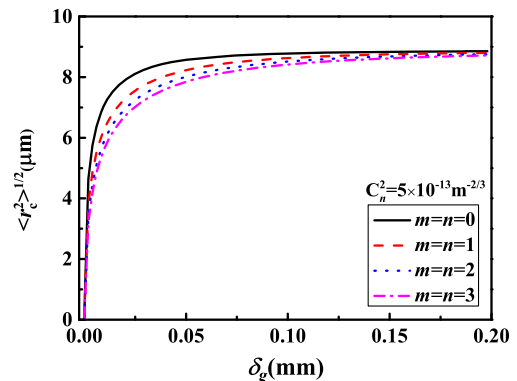

Fig. 1. Beam wander of HGCSM beams in the receiver plane versus coherence length for different beam orders.
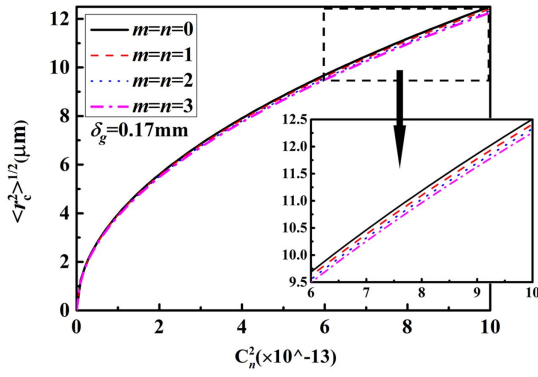
Fig. 2. Beam wander of HGCSM beams in the receive plane versus the generalized refractive-index structure parameter for different beam orders.

later experimental results, though it can be seen in Fig. 1 that a smaller δ_g results in a more significant effect. We first note that the value of the beam wander increases rapidly with the increase in C_n^2. For larger values of C_n^2, the dependence becomes linear. Figure 2 also illustrates that the beam wander of HGCSM beams decreases as the order of the beams increases.

Next, we compare the experimental beam wander of HGCSM beams with our theoretical results. Figure 3 shows our experimental setup, including both the generation of a HGCSM beam as well as the measurement of both the source spatial coherence and beam wander after thermally induced turbulence. A laser beam emitted from a He–Ne laser ($\lambda = 632.8$ nm) first passes through a neutral density filter (NDF) and then goes through a beam expander (BE). After being redirected by a reflecting mirror (RM), the laser goes toward a spatial light modulator (SLM), which acts as a phase grating designed by the method of computer-generated holograms. We then select the first-order diffraction pattern of the holograms with a circular aperture (CA). The beam from the CA first passes through a thin lens L_1 and then illuminates a rotating ground-glass disk (RGGD), producing an incoherent beam. After passing through a collimated thin lens L_2 and a Gaussian amplitude filter (GAF) ($\sigma_0 = 2.5$ mm), a HGCSM beam is generated just behind the GAF, i.e., the plane behind the GAF is the source plane $z = 0$.

The generated source is further split into two components by a beam splitter (BS). The reflected part passes through a lens L_3 with focal length f_3 and arrives at a charge-coupled device (CCD$_1$), which can record the instantaneous intensity. The distance from the GAF to L_3 is equal to the distance from L_3 to the CCD$_1$, and the distance is $2f_3$ (i.e., it is a $4f$ imaging system); thus, the spatial coherence width in the image plane of CCD$_1$ is the same as that in the source plane. We can measure
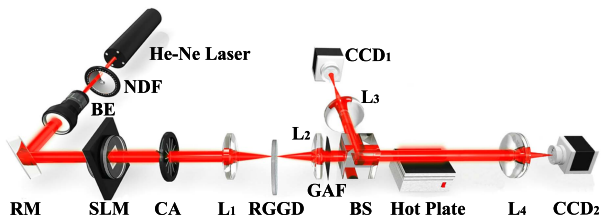
the spatial coherence width of the generated beam through the frames captured (instantaneous intensity) by CCD$_1$. The measuring process and the related derivation of the spatial coherence width were reported in a previous paper and can be found in Ref. [27]. The transmitted beam passes over a 35 cm × 50 cm electric hot plate and then through a collecting lens L_4, then arrives at CCD$_2$, located in the focal plane of L_4. The CCD$_2$ records the instantaneous intensity distribution, and the output signal is sent to a computer to calculate beam wander. The distance from GAF (source plane) to L_4 is 2.5 m and the electric hot plate is located between the GAF and L_4. The electric hot plate produces turbulence through convection, and the strength of the turbulence is controlled by the temperature of the hot plate. The beam center is about 2.5 cm above the hot plate surface.

One important consideration in the experimental measurement of beam wander is the relative sizes of characteristic times of the system, namely, the characteristic time τ_s of the intensity fluctuations induced by the RGGD, the characteristic time τ_a of the intensity fluctuations induced by turbulence, and the integration time τ_d of the CCD$_2$. In most previous theoretical studies of beam wander [6,25,28], the detector is assumed to be a "slow" detector, and the times satisfy the inequality $\tau_s \ll \tau_d \ll \tau_a$. Thus, the CCD$_2$ in our experiment is regarded as a slow detector, and it is sensitive to the turbulence-induced wander, but not the source fluctuations caused by the RGGD.

We evaluate the value of the beam wander $\langle r_c^2 \rangle^{1/2}$ in the receiver plane from the data by the following formula [7]:

$$\langle r_c^2 \rangle^{1/2} = \left[\sum_{n'=1}^{N} \frac{(x_{n'} - \bar{x}_c)^2 + (y_{n'} - \bar{y}_c)^2}{N} \right]^{1/2}, \quad (8)$$

where N is the number of total frames recorded by the CCD$_2$. In this experiment, we recorded 3000 frames, i.e., $N = 3000$. The vector $(x_{n'}, y_{n'})$ denotes the spatial coordinates of the centroid of each frame, and n' denotes number of realizations, ranging from 1–3000. The vector $(\bar{x}_c, \bar{y}_c)$ represents the average coordinates of the centroid of total frames. They satisfy the formulas

$$x_{n'} = \sum_i \sum_j x_i I_{n'}(x_i, y_j) / \sum_i \sum_j I_{n'}(x_i, y_j), \quad (9)$$

$$y_{n'} = \sum_i \sum_j y_j I_{n'}(x_i, y_j) / \sum_i \sum_j I_{n'}(x_i, y_j), \quad (10)$$

$$\bar{x}_c = \sum_i \sum_j x_i I_t(x_i, y_j) / \sum_i \sum_j I_t(x_i, y_j), \quad (11)$$

$$\bar{y}_c = \sum_i \sum_j y_j I_t(x_i, y_j) / \sum_i \sum_j I_t(x_i, y_j), \quad (12)$$

where $I_{n'}(x_i, y_j)$ denotes the intensity of the n'th frame, and $I_t(x_i, y_j)$ denotes the total intensity distribution found by summing over the 3000 realizations. The pair (x_i, y_j) is the pixel spatial coordinates of the frames.

Using Eq. (8), we can measure the beam wander of HGCSM beams and study its dependence on the initial beam coherence width and the temperature of the hot plate, for different beam orders.

Figure 4 shows the experimental beam wander of HGCSM beams in the receiver plane versus the coherence width δ_g, when

Fig. 3. Experimental setup for generating and measuring spatial coherence width and beam wander of a HGCSM beam.
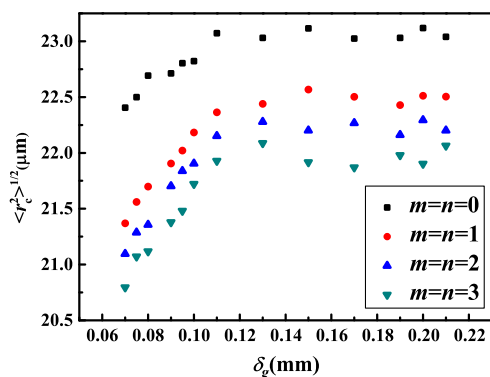
Fig. 4. Experimental results of beam wander of generated HGCSM beams in the receiver plane versus coherence width for different beam orders.
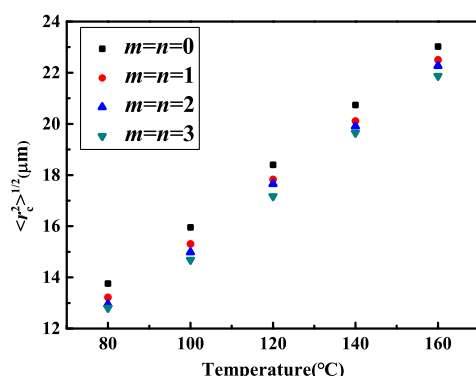

Fig. 5. Experimental results for beam wander of generated HGCSM beams in the receiver plane versus the temperature of the hot plate for different beam orders.

the temperature of the hot plate is 160°C, for different values of beam orders m and n. It is seen that the value of the beam wander increases rapidly with an increase in δ_g when the value of δ_g is smaller than 0.11 mm. The value of the beam wander is almost independent of the coherence width δ_g when the value of δ_g is larger than 0.11 mm. Furthermore, we note that the beam wander of a HGCSM beam with large beam orders m and n is smaller than that of a HGCSM beam with small m and n or a GSM beam, which means that a high-order HGCSM beam is less affected by thermal turbulence, at least with respect to beam wander; these results can be compared to Fig. 1.

Figure 5 shows the experimental beam wander of HGCSM beams versus the temperature of the hot plate for different beam orders. We find that the value of the beam wander increases almost linearly with an increase in the temperature of the hot plate (i.e., the strength of turbulence). We can also confirm from Fig. 5 that a HGCSM beam is less affected by the turbulence than a GSM beam and that increasing the beam orders of HGCSM beams will enhance the ability of turbulence resistance; these results can be compared to Fig. 2.

It is clear from the figures that the experimental results verify the functional behavior of the theoretical model, and the superior performance of higher-order HGCSM beams. We believe that the discrepancy in the details between theoretical and experimental results is caused by differences between our simple theoretical turbulence model and actual experimental turbulence. In the experiment, the exact model for the power density spectrum is unknown and likely differs from the von Karman power spectrum used for the theoretical calculation.

Through both theoretical and experimental studies, we confirm that the use of HGCSM beams of low coherence and high order provides one way to reduce turbulence-induced beam wander for a given beam size. The essence of reducing beam wander is an increase in the beam size in the receiving plane. For different cases with the same beam size in the receiving plane, the beam wander is smaller for a larger source beam size. Our results show that modulating the coherence structure of structured light beams is a very effective strategy to reduce the negative effects of turbulence, an insight that will be useful in free-space optical communications.

REFERENCES

1. L. C. Andrews and R. L. Phillips, *Laser Beam Propagation in the Turbulent Atmosphere* (SPIE, 2005).
2. L. C. Andrews, R. L. Phillips, R. J. Sasiela, and R. R. Parenti, Opt. Eng. **45**, 076001 (2006).
3. B. Zhang, Y. Xu, X. Wang, and Y. Dan, OSA Continuum **2**, 162 (2019).
4. V. Usenko, C. Peuntinger, B. Heim, K. Günthner, I. Derkach, D. Elser, C. Marquardt, R. Filip, and G. Leuchs, Opt. Express **26**, 31106 (2018).
5. R. Calvo, D. Calia, R. Barrios, M. Centrone, D. Giggenbach, G. Lombardi, P. Beckera, and I. Zayer, Proc. SPIE **10096**, 10096 (2017).
6. G. P. Berman, A. A. Chumak, and V. N. Gorshkov, Phys. Rev. E **76**, 056606 (2007).
7. X. Liu, F. Wang, C. Wei, and Y. Cai, Opt. Lett. **39**, 3336 (2014).
8. W. Wen and X. Chu, J. Mod. Opt. **61**, 379 (2014).
9. Y. Huang, Y. Yuan, X. Liu, J. Zeng, F. Wang, J. Yu, L. Liu, and Y. Cai, Appl. Sci. **8**, 2476 (2018).
10. G. Gbur and E. Wolf, J. Opt. Soc. Am. A **19**, 1592 (2002).
11. T. Shirai, A. Dogariu, and E. Wolf, J. Opt. Soc. Am. A **20**, 1094 (2003).
12. Y. Huang, A. Zeng, Z. Gao, and B. Zhang, Opt. Lett. **40**, 1619 (2015).
13. G. Wu, W. Dai, H. Tang, and H. Guo, Opt. Commun. **336**, 55 (2015).
14. S. Yu, Z. Chen, T. Wang, G. Wu, H. Guo, and W. Gu, Appl. Opt. **51**, 7581 (2012).
15. Y. Cai, Y. Chen, and F. Wang, J. Opt. Soc. Am. A **31**, 2083 (2014).
16. Y. Cai, Y. Chen, J. Yu, X. Liu, and L. Liu, Prog. Opt. **62**, 157 (2017).
17. H. Lajunen and T. Saastamoinen, Opt. Lett. **36**, 4104 (2011).
18. Z. Mei and O. Korotkova, Opt. Lett. **38**, 91 (2013).
19. Y. Chen, J. Gu, F. Wang, and Y. Cai, Phys. Rev. A **91**, 013823 (2015).
20. J. Yu, F. Wang, L. Liu, Y. Cai, and G. Gbur, Opt. Express **26**, 16333 (2018).
21. J. Yu, Y. Cai, and G. Gbur, Opt. Express **26**, 27894 (2018).
22. Y. Gu and G. Gbur, Opt. Lett. **38**, 1395 (2013).
23. X. Liu, J. Yu, Y. Cai, and S. A. Ponomarenko, Opt. Lett. **41**, 4182 (2016).
24. J. Yu, Y. Chen, L. Liu, and Y. Cai, Opt. Express **23**, 13467 (2015).
25. X. Xiao and D. G. Voelz, Opt. Eng. **51**, 026001 (2012).
26. Y. Dan and B. Zhang, Opt. Lett. **34**, 563 (2009).
27. C. Liang, F. Wang, X. Liu, Y. Cai, and O. Korotkova, Opt. Lett. **39**, 769 (2014).
28. D. G. Pérez and G. Funes, Opt. Express **20**, 27766 (2012).